Additional Information

Geometrical definition of a continuous family of time transformations on the hyperbolic two-body problem.

José A. López Ortí*†[1], Francisco José Marco Castillo †
and María José Martínez Usó ‡

† Departamento de Matemáticas. IMAC. Universidad Jaume I.
Av Sos Baynat s/n. E-12071 Castellón. Spain

‡ Departamento de Matemática Aplicada. IUMPA. Universidad Politécnica de
Valencia.
Camino Vera s/n. E-46022 Valencia. Spain

lopez.at.mat.uji.es, marco.at.mat.uji.es, mjmartin.at.mat.upv.es

Abstract

This paper is aimed to address the study of techniques focused on the use of a family of anomalies based on a family of geometric transformations depending on a parameter α that includes the true anomaly. This family is an extension of the elliptic geometrical transformation at the hyperbolic case.

This family allows to get closed equations for the classical quantities of the hyperbolic two body problem both in the attractive and in the repulsive case.

In this paper we obtain the link between hyperbolic funtions of hyperbolic argument H with trigonometric funtions for each temporal variable in the new family. This study includes also the inverse relations. This paper includes in the attractive case the study of the minimization of the errors due to the choice of the a temporal variable include in our family in the numerical integration by an appropriate choice of parameters. This study includes the analysis the dependence on the parameter of integration errors in a great time span for several eccentricities and the study of local truncation errors in the region with true anomaly contained in the intervall $[-\pi/2, \pi/2]$ around the primary for several values of the parameter.

Keywords: Celestial mechanics. Orbital motion. Ordinary differential equations. Computational algebra.
2000 MSC: 70F05, 70F10, 70F15,70M20.

1. Introduction

One of the most important topics in celestial mechanics is the study of the two-body problem. This problem includes the elliptic, parabolic and hyperbolic motions and its solution can be described through the orbital elements, for

example the third set of Brouwer and Clemence [1] $(a, e, i, \Omega, \omega, M)$ in the elliptic and hyperbolic case. The parabolic case is a limit case when $e = 1$ and the major semiaxis is infinite and so it can be replaced by the parameter p. The elliptic motion is the most important case because it can be used to obtain a first approximation to the motion of the planets, natural and artificial satellites, periodic comets, etc.

The parabolic motion is an extreme case that separates the regions of elliptical and hyperbolic motion. Parabolic motion is appropriate as a first approximation to the orbit of celestial bodies with eccentricity close to unity in the perihelion region. In this case, from a few observations we can determine a provisional parabolic orbit and then we can make a short term tracking of the body to obtain more positions in order to improve the accuracy of its orbital elements. In particular its eccentricity even if it is a periodic comet so the method does not depend on the form of the orbit (elliptical if it is periodic).

While, in general, the hyperbolic motion is less important in celestial mechanics than the elliptical case, it has a special interest in problems of astronautics where in many occasions the gravitational force of the planets can be used to move the spacecraft during a time in an hyperbolic orbit around them to direct the spacecraft to its target.

To study of motion of the spacecraft in hyperbolic motion it is appropriate the use of the numerical integrators and, as in the elliptical case, the performance is good, although an adequate choice of the temporal variable can, in certain cases, increase the efficiency of these methods. The use of the natural time as integration variable presents in the hyperbolic case a problem that becomes greater when the eccentricity approaches one. The problem is that at temporal regular intervals there is much lower concentration of points in the region of the periapsis in which velocity and curvature are maxima than in remote regions where the motion is quasi inertial.

The relative motion of the secondary with respect to the primary is defined by the second order differential equations

$$\frac{d^2\vec{r}}{dt^2} = -\mu\frac{\vec{r}}{r^3} + \vec{F} \tag{1}$$

where $\vec{r}$ is the radius vector of the secondary, μ is the spaceflight constant given by $\mu = G(M + m)$ in the gravitatory case where G is the gravitational constant, and M, m the masses of primary and secondary respectively and $\vec{F}$ the perturbative forces.

In the electrostatic case we have $\mu = \left(K\frac{Q}{M}\frac{q}{m} - G\right)(M + m)$ where Q and q are the charges of primary and secondary body, M and m their masses and K is the Coulombian constant. In general, in this case, we can ignore the gravitatory forces ($|G| << K$) and also the magnetic forces when $v^2/c^2 << 1$. In the case of the electrostatic forces they are repulsive when the charges of two bodies are of same sign and attractive when signs of electric charges are opposite.

To integrate the system (1) it is necessary to know the initial values of the radius vector $\vec{r}_0$ and velocity $\vec{v}_0$

The hyperbolic motion in its external branch describes the solution of relative motion of a pair of electric charges with the same sign and it is interesting to study problems such as scattering by dispersion. In this case also in the periapsis, region the secondary is submitted to major forces and in this region then density of points is lower if natural time is used.

In order to uniformize the truncation errors when a numerical integrator is used there are three main techniques:

1. The use of a very small stepsize.
2. The use of an adaptative stepsize method.
3. The use of a change in the temporal variable to arrange an appropriate distribution of the points on the orbit so that the points are mostly concentrated in the regions where the acceleration and curvature are maxima.

This paper follows the third technique. Several authors have already studied this question for the elliptic motion, starting from the Sundman transformation [10], introducing a new temporal variable τ related to the time t through $dt = Cr d\tau$. Other transformations are proposed by Nacozy [9], Brumberg [2] proposed the use of the regularized length of arc and Brumberg and Fukushima [3] introduced the elliptic anomaly as temporal variable. Janin [5], [6] and Velez [11] generalized Sundman transformations $dt = C_\alpha r^\alpha d\tau_\alpha$, Ferrandiz [4] introduces the generalized elliptic anomaly, López [7] introduces an new family of anomalies, called natural anomalies and López defines a geometrical family of transformations that includes the true anomaly f, the eccentric anomaly g and the antifocal anomaly f'. These transformations are defined as $dM = Q(r)d\Psi$ where $M = n(t - t_0)$ is the mean anomaly, $n = \sqrt{|\mu|/a^3}$ the fictitious mean motion t the time, t_0 the epoch of periapsis transit, Ψ the new anomaly derived from the change in the temporal variable and $Q(r)$ is a function of the vector radius r called partition function.

The geometrical family of continuous transformations [8] for the elliptic case presents good properties such as closed formulas for the most common quantities of the two body problem, closed form in the coefficients of Fourier developments used in the analytical theories of the perturbed motion and an appropriate performance in the numerical methods. In this paper we try to extend this family of transformations to hyperbolic attractive and repulsive motion in order to obtain the most important quantities of the two body problem with respect these new variables. This work includes a initial study of the dependence on the new variables of the integration errors in numerical methods.

The rest of this paper is organized as follows: In this section the general background has been introduced. In section 2 the properties of generalized geometic family of anomalies will be described. In particular, we will obtain the most common quantities of the problem in closed form using an arbitrary anomaly from this family for the hyperbolic atractive case. In section 3, following a similar way, we extend the analytical study to hyperbolic repulsive case obtaining closed formulas. In section 4 a set of numerical examples about the atractive hyperbolic two body problem will be considered. In section 5 the main conclusions and remarks will be exposed.

2. Generalized geometric anomalies

In this section a new family of anomalies depending on one parameter is defined. We represent in figure 1 the hyperbolic orbit corresponding to the motion of the gravitational two body problem. This hyperbola is defined by its major semiaxis $a = \overline{OQ}$ and its eccentricity $e = \frac{c}{a}$, $1 < e$ where c is the focal semidistance, and the minor semiaxis b is defined as $b = a\sqrt{e^2 - 1}$. Let F_{eq} be the focus position of equilateral hyperbola with the same center and major semiaxis that the orbit, F the primary focus and O the center of the hyperbola.

Let us define F_α as the point of coordinates $(-\alpha\, e\, a, 0)$, $\alpha \in]\frac{1}{e}, 1]$, Q the periapsis and P the position of the secondary in the orbit. The point F_α is the primary focus of an hyperbola with the same center and major semiaxis as the orbit and the minor semiaxis $\overline{OF_\alpha} = \alpha\, e\, a$ where e is the eccentricity of the orbit and $\alpha \in [\frac{1}{e}, 1]$. Notice that $F_\alpha = F_{eq}$ if $\alpha = \sqrt{2}$ and $F_\alpha = F$ if $\alpha = 1$. Let us define the orbital coordinates (ξ, η) referred to the primary focus, and let r be the distance between the secondary P and the primary focus F. The equilateral hyperbola with center O and semiaxis OQ can be parametrized referred to the center as $x = -a\cosh H$, $y = a\sinh H$ where H is called hyperbolic argument, the angle f is called true anomaly.

In figure 1 we introduce following [8] the anomalies $\Psi_\alpha = \widehat{OF_\alpha P_\alpha}$. Notice that for $\alpha = 1$ we have the true anomaly f.

The motion of the secondary with respect to the primary is related to the true anomaly f and the argument H as

$$\xi = r\cos f = a(e - \cosh H), \quad \eta = r\sin f = a\sqrt{e^2 - 1}\sinh H, \qquad (2)$$

ad so

$$r = a(e\cosh H - 1) \qquad (3)$$

where $r = \overline{FP}$ is the vector radius of the secondary P with respect to the primary F and its value is given by

$$r = \frac{a(e^2 - 1)}{1 + e\cos f}, \quad f \in]-\arccos\frac{-1}{e}, \arccos\frac{-1}{e}[. \qquad (4)$$

To study the hyperbolic motion it is convenient to introduce the fictitious mean motion $n = \sqrt{\mu/a^3}$ where $\mu = GM$ is the spaceflight constant and the mean anomaly $M = n(t - t_0)$, where $t_=$ is the epoch of the transit for the periapsis. The mean anomaly is connected to the hyperbolic argument trough the Kepler equation:

$$e\sinh H - H = M, \qquad (5)$$

and the true anomaly f is linked to the hyperbolic argument by means of

$$\tan\frac{f}{2} = \sqrt{\frac{e+1}{e-1}}\tanh\frac{H}{2} \qquad (6)$$

In figure 1 we see P the position of the secondary on the orbit, P_α the orthogonal projection on hyperbola with the same major semiaxis and eccentricity αe of P_e the point corresponding on the equilateral hyperbola in the
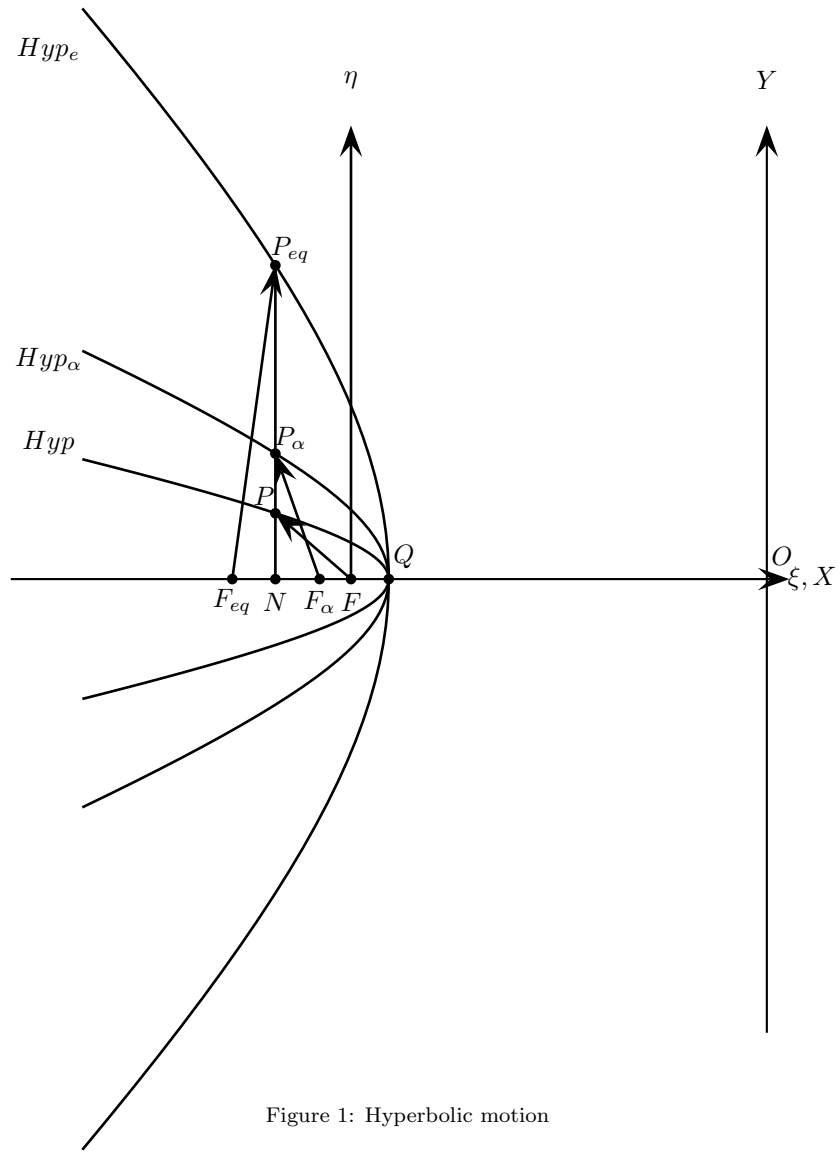
4

Figure 1: Hyperbolic motion

family ($\alpha = \sqrt{2}$) and N the projection on the major semi-axis. In this family of hyperbolas we have the relationship:

$$\frac{\overline{NF_\alpha}}{b_\alpha} = \frac{\overline{NP_e}}{a} = \frac{\overline{NP}}{b} \tag{7}$$

where $b = a\sqrt{e^2 - 1}$ is the minor semiaxis of the hyperbola, a the major semi-axis and $b_\alpha = a\sqrt{\alpha^2 e^2 - 1}$ the minor semiaxis corresponding to the hyperbola with eccentricity αe. The vector radius of point $\overrightarrow{F_\alpha P_\alpha}$ is defined by its module r_α and the value of the anomaly Ψ_α. The radius r_α is related to Ψ_α through:

$$r_\alpha = \frac{a(\alpha^2 e^2 - 1)}{1 + \alpha e \cos \Psi_\alpha}. \tag{8}$$

Analogously, it is related to H through the equation:

$$r_\alpha = a(\alpha\, e \cosh H - 1) \tag{9}$$

and so

$$r_\alpha = \alpha\, r + (1 - \alpha)(-a) \tag{10}$$

On the other hand $\overline{OF} = a\,e$, $\overline{OF_\alpha} = \alpha\, a\, e$ and, taking into account (7), the coordinates (ξ, η) of the secondary are related to Ψ_α through:

$$\xi = r_\alpha \cos \Psi_\alpha + ae(1 - \alpha), \quad \eta = \frac{\sqrt{e^2 - 1}}{\sqrt{\alpha^2 e^2 - 1}} r_\alpha \sin \Psi_\alpha \tag{11}$$

and so

$$\xi = a\left[\frac{(\alpha^2 e^2 - 1)\cos \Psi_\alpha}{1 + \alpha e \cos \Psi_\alpha} + (1 - \alpha)e\right], \quad \eta = a\sqrt{\frac{e^2 - 1}{\alpha^2 e^2 - 1}} \frac{(\alpha^2 e^2 - 1)\sin \Psi_\alpha}{1 + \alpha e \cosh \Psi_\alpha}. \tag{12}$$

To link H with Ψ_α we consider the classical relations and operating we have

$$\cos \Psi_\alpha = \frac{\alpha\, e - \cosh H}{\alpha\, e \cosh H - 1}, \tag{13}$$

and

$$\sin \Psi_\alpha = \frac{\sqrt{\alpha^2 e^2 - 1}\, \sinh H}{\alpha\, e \cosh H - 1}, \tag{14}$$

and from (13), (14) it is easy to get

$$\cosh H = \frac{\alpha\, e + \cos \Psi_\alpha}{1 + \alpha\, e \cos \Psi_\alpha}, \tag{15}$$

and

$$\sinh H = \frac{\sqrt{\alpha^2 e^2 - 1}\, \sin \Psi_\alpha}{1 + \alpha\, e \cos \Psi_\alpha}. \tag{16}$$

To evaluate the orbital velocity with respect to the anomaly Ψ_α we consider the well-known equations

$$\dot{\xi} = \frac{na\sinh H}{e\cos H - 1} \quad , \dot{\eta} = \frac{na\sqrt{e^2-1}\cosh H}{e\cosh H - 1}, \tag{17}$$

and taking into account (15) and (16) we obtain

$$\dot{\xi} = -\frac{na\sqrt{\alpha^2 e^2 - 1}\sin\Psi_\alpha}{\alpha e^2 - 1 + (1-\alpha)e\cos\Psi_\alpha}, \quad \dot{\eta} = \frac{na\sqrt{e^2-1}(\cos\Psi_\alpha + \alpha e)}{\alpha e^2 - 1 + (1-\alpha)e\cos\Psi_\alpha}, \tag{18}$$

Finally, replacing (15) in the classical equation $r = a(e\cosh H - 1)$, we have for the vector radius

$$r = a\frac{(\alpha\, e^2 - 1) + e(1-\alpha)\cos\Psi_\alpha}{1 + \alpha\, e\cos\Psi_\alpha}, \tag{19}$$

The anomaly Ψ_α is related to the hyperbolic argument H by means of:

$$\tan\frac{\Psi_\alpha}{2} = \sqrt{\frac{\alpha\, e + 1}{\alpha\, e - 1}}\tanh\frac{H}{2}. \tag{20}$$

To connect $d\Psi_\alpha$ and dM we derivate (14)

$$\cos\Psi_\alpha d\Psi_\alpha = \frac{\sqrt{\alpha^2 e^2 - 1}(\alpha\, e - \cosh H)}{(\alpha\, e\cosh H - 1)(\alpha\, e\cosh H)^2}dH, \tag{21}$$

and, taking into account (13) we obtain

$$d\Psi_\alpha = \frac{\sqrt{\alpha^2 e^2 - 1}\,dH}{\alpha\, e\cosh H}, \tag{22}$$

replacing in this equation (19) we get

$$d\Psi_\alpha = \sqrt{\alpha^2 e^2 - 1}\frac{a}{r_\alpha}dH, \tag{23}$$

and taking into account the hyperbolic Kepler equation (5) we have

$$dH = \frac{a}{r}dM, \tag{24}$$

we obtain

$$dM = \frac{r r_\alpha}{a^2\sqrt{\alpha^2 e^2 - 1}}d\Psi_\alpha, \tag{25}$$

which can be written as $dM = Q(r)d\Psi_\alpha$ where $Q(r)$ is the partition function

$$Q(r) = \frac{r\, r_\alpha}{a^2\sqrt{\alpha^2 e^2 - 1}} = \frac{r(1-\alpha)(-a) + \alpha\, r^2}{a^2\sqrt{1 - \alpha^2 e^2}}, \tag{26}$$

notice that the partition function $Q(r)$ is symmetric in its first form.
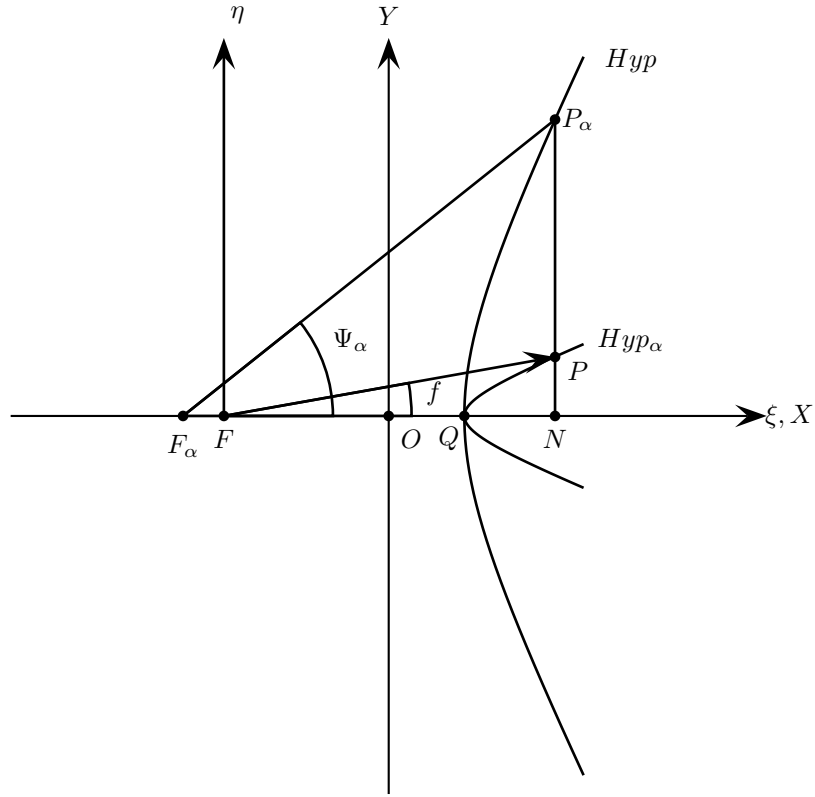
7

Figure 2: Hyperbolic motion

3. Hyperbolic repulsive motion

In the case of central repulsive forces in the form $\vec{F} = \mu \frac{\vec{r}}{r^3}$, $\mu > 0$ the motion referred to the primary satisfies the second Kepler law and it is hyperbolic. The secondary describes the external branch of the hyperbola with focus on the primary. In this case (figure 2), if we define the coordinate system (ξ, η) cantered on the primary F the coordinate ξ runs to the periapsis and the coordinate η forms a direct oriented coordinate system with ξ. Let O be the centre of the hyperbola and the coordinate system OXY defined by the direction of the secondary focus and the axis OY orthogonal to OX. The coordinates (x, y) are related to (ξ, η) through $\xi = x + a\,e$, $y = \eta$ where a is the semimajor axis of the hyperbola and e is its eccentricity. Let H be a variable called hyperbolic argument, the parametric equation of the external branch of the hyperbola can be obtained as

$$x = a \cosh H, \quad y = a\sqrt{e^2 - 1} \sinh H, \tag{27}$$

8

and so
$$\xi = a(\cosh H + e), \quad \eta = a\sqrt{e^2 - 1}\sinh H, \tag{28}$$

and so
$$r = a(e\cos H + 1). \tag{29}$$

Let P be the position of the secondary, f the true anomaly and $\vec{r}$ the vector radius of the secondary $\vec{r} = \overline{FP}$. The coordinates (ξ, η) can be written as
$$\xi = r\cos f, \ \eta = r\sin f, \tag{30}$$

where r is given by
$$r = -\frac{a(e^2 - 1)}{1 - e\cos f}, \ H \in \mathbb{R}, \ f \in\,] -\arccos\frac{1}{e}, \arccos\frac{1}{e}[. \tag{31}$$

The true anomaly f is related to the hyperbolic argument H through
$$\tan\frac{f}{2} = \sqrt{\frac{e-1}{e+1}}\tanh\frac{H}{2}. \tag{32}$$

The Kepler equation in this case can be written as
$$e\sinh H + H = M. \tag{33}$$

The coordinates (ξ, η) are related to Ψ_α by
$$\xi = r_\alpha\cos\Psi_\alpha - a\,e(\alpha - 1) \tag{34}$$
$$\eta = \sqrt{\frac{e^2 - 1}{\alpha^2 e^2 - 1}}r_\alpha\sin\Psi_\alpha$$

where r_α is given by
$$r_\alpha = a(\alpha\,e\cos H + 1), \tag{35}$$

and with repect to Ψ_α
$$r_\alpha = -\frac{a(\alpha^2\,e^2 - 1)}{1 - \alpha\,e\cos\Psi_\alpha}. \tag{36}$$

From (35) it is easy to obtain
$$r_\alpha = \alpha r + (1 - \alpha)a. \tag{37}$$

To connect H with Ψ_α we have from (28), (34) and (35)
$$\cosh H = \frac{\cos\Psi_\alpha - \alpha\,e}{1 - \alpha\,e\cos\Psi_\alpha}, \tag{38}$$

and
$$\sinh H = -\frac{\sqrt{\alpha^2 e^2 - 1}\sin\Psi_\alpha}{1 - \alpha\,e\cos\Psi_\alpha}. \tag{39}$$

9

From (38) and (39) it is easy to get

$$\cos \Psi_\alpha = \frac{\alpha\, e + \cosh H}{1 + \alpha\, e \cosh H}, \tag{40}$$

and

$$\sin \Psi_\alpha = \frac{\sqrt{\alpha^2 e^2 - 1}\, \sinh H}{1 + \alpha\, e \cosh H}. \tag{41}$$

The anomaly Ψ_α is linked to H by

$$\tan \frac{\Psi_\alpha}{2} = \sqrt{\frac{\alpha\, e - 1}{\alpha\, e + 1}}\, \tanh \frac{H}{2}. \tag{42}$$

Finally, to link $d\Psi_\alpha$ with dM we derivate (39)

$$\cosh H\, dH = -\sqrt{\alpha^2 e^2 - 1}\, \frac{\cos \Psi_\alpha - \alpha\, e}{(1 - \alpha\, e \cos \Psi_\alpha)^2}\, d\Psi_\alpha, \tag{43}$$

and taking into account (36) we get

$$dH = \frac{r_\alpha}{a\sqrt{\alpha^2 e^2 - 1}}\, d\Psi_\alpha. \tag{44}$$

Derivating the Kepler equation (33) we obtain $dM = \frac{r}{a} dH$ and so

$$dM = \frac{r\, r_\alpha}{a^2 \sqrt{\alpha^2 e^2 - 1}}\, d\Psi_\alpha. \tag{45}$$

From this equation we have $dM = Q(r) d\Psi_\alpha$ where $Q(r)$ is the partition function. Notice that this form coincides in the attractive and repulsive motion.

$$Q(r) = \frac{r\, r_\alpha}{a^2 \sqrt{\alpha^2 e^2 - 1}} = \frac{r(\alpha\, r + (1 - \alpha)a)}{a^2 \sqrt{\alpha^2 e^2 - 1}} \tag{46}$$

Notice that the partition function $Q(r)$ in its first form is symmetric and coincides in both the attractive and repulsive motion.

4. Numerical examples

In general, the perturbative forces are small, for this reason it is convenient to test the numerical methods applying them to the well-known two body problem, referred to the orbital coordinate system $(x, y, 0) = (\xi, \eta, 0)$. In order to select an appropriate new temporal variable with the aim of minimizing the distribution of the truncation errors on the orbit, let us define a generic family Ψ_α of anomalies depending on a parameter α as $dt = Q_\alpha(r) d\Psi_\alpha$, for each α we have

$$\frac{d}{dt} = n \frac{d}{dM} = n \frac{d}{d\Psi_\alpha} \frac{d\Psi_\alpha}{dM} = \frac{n}{Q_\alpha(r)} \frac{1}{d\Psi_\alpha} \tag{47}$$

so

$$\frac{dx}{d\Psi_\alpha} = \frac{Q_\alpha(r)}{n} v_x, \quad \frac{dv_x}{d\Psi_\alpha} = -\frac{Q_\alpha(r)}{n} \left[GM\frac{x}{r^3} + \frac{\partial V}{\partial x} - F_x \right]$$

$$\frac{dy}{d\Psi_\alpha} = \frac{Q_\alpha(r)}{n} v_y, \quad \frac{dv_y}{d\Psi_\alpha} = -\frac{Q_\alpha(r)}{n} \left[GM\frac{y}{r^3} + \frac{\partial V}{\partial y} - F_y \right] \qquad (48)$$

In order to evaluate the performance of this method we use for the test a ficti-
tious body with major semiaxis $a = 118363.47 Km$ in hyperbolic motion around
a mass 10^5 times greater than the Earth. The motion is studied on its orbital
plane using several anomalies in our family, the aim is not to obtain the best
integrator instead, our purpose is to study the errors dependence on Ψ_α. To
this aim, we perform two numerical experiments: in the first place a numeri-
cal experiment evaluating the dependence on α value of the errors in a great
time span. In the second place, the study of the local truncation errors in an
extreme case of eccentricity $e = 1.05$ in a region near the periapsis defined by
$f \in [-\pi/2, \pi/2]$, where f is the true anomaly.

Integration errors for the selected anomaly Ψ_α depend on the point distri-
bution on the hyperbola. In Figure 3 we show a sample of twenty points for Ψ_α
with homogeneous distribution on the orbit for several anomalies for a hyperbola
with eccentricity $e = 1.5$.

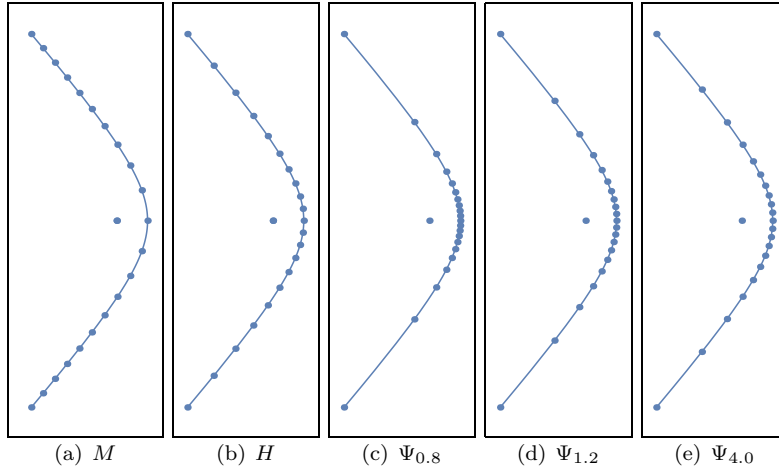| (a) M | (b) H | (c) $\Psi_{0.8}$ | (d) $\Psi_{1.2}$ | (e) $\Psi_{4.0}$ |

Figure 3: Points distribution for M, H, $\Psi_{0.8}$, $\Psi_{1.2}$ $\Psi_{4.0}$

The first numerical experiment has been carried out by the study of position
error value given by $\Delta r = \sqrt{(x_i - x_f)^2 + (y_i + y_f)^2}$ in Km, where the initial
condition is the value of (x, y), coordinates for the fictitious mean anomaly
$M = -50$, and (x_f, y_f) the value obtained for $M = 50$ using the constant step

11

size classic Runge-Kutta method of 4th order with $h = 0,005$ for several values of eccentricity. Figure 3 shows that the value of error decreases when α increases and this value tends to stabilize. In this figure, the OX and OY axis represent the value of α and $\log_{10} \Delta r$, respectively.
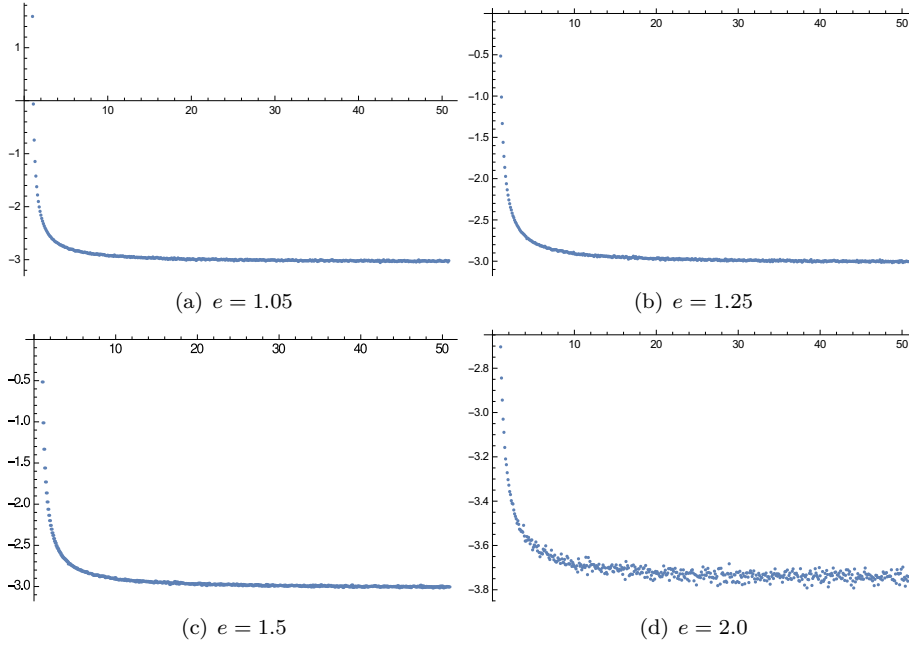

(a) $e = 1.05$

(b) $e = 1.25$

(c) $e = 1.5$

(d) $e = 2.0$

Figure 4: Integration errors distribution for several values of e in function of α

The second numerical experiment consists in the study of the local integration errors, in Km for the position and Km/s for the velocity, for a satellite with $a = 118363.47Km$, eccentricity $e = 1.05$ and spaceflight constant $\mu = GM = 3.9860044151\dot{1}0^{10}$, using as temporal variable the mean anomaly M and the Ψ_{alpha} anomalies for the values of $\alpha = 1.00, 2.00, 5.00$. These errors have been obtained by comparison of the values obtained integrating one step the differential equations (48) with the initial conditions given by (12) and , for each $\Psi_\alpha = i \cdot h$ where $h = |\Psi_{\alpha_0}|/100$, $i = 0, \ldots, 200$ with the exact results obtained from (12) and , for $\Psi_\alpha = (i + 1)h$, where Ψ_{α_0} is the value of Ψ_α for $f = -\pi/2$. In the case of M the initial value M_0 is obtained from the value of H_0 given by (6) for $f = -\pi/2$ and we follow a similar procedure. Figures 5,6,7,8 show the local integration errors in the coordinate (x, y) in Km and velocities (v_x, v_y) in Km/s obtained in this experiment.
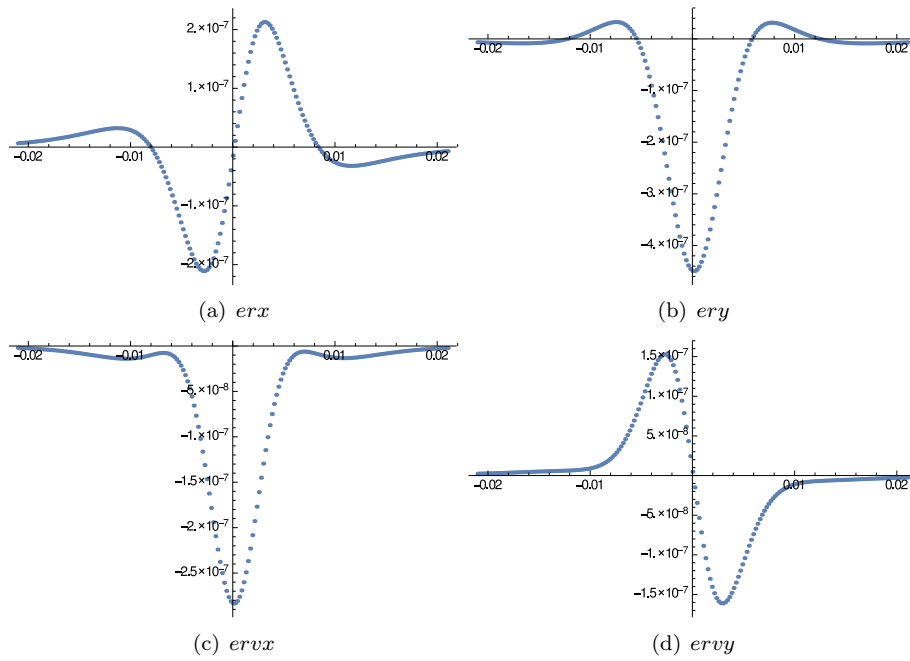
(a) *erx*

(b) *ery*

(c) *ervx*

(d) *ervy*

Figure 5: Local integration errors distribution $e = 1.05$, and M

13

(a) *erx*

(b) *ery*

(c) *ervx*

(d) *ervy*
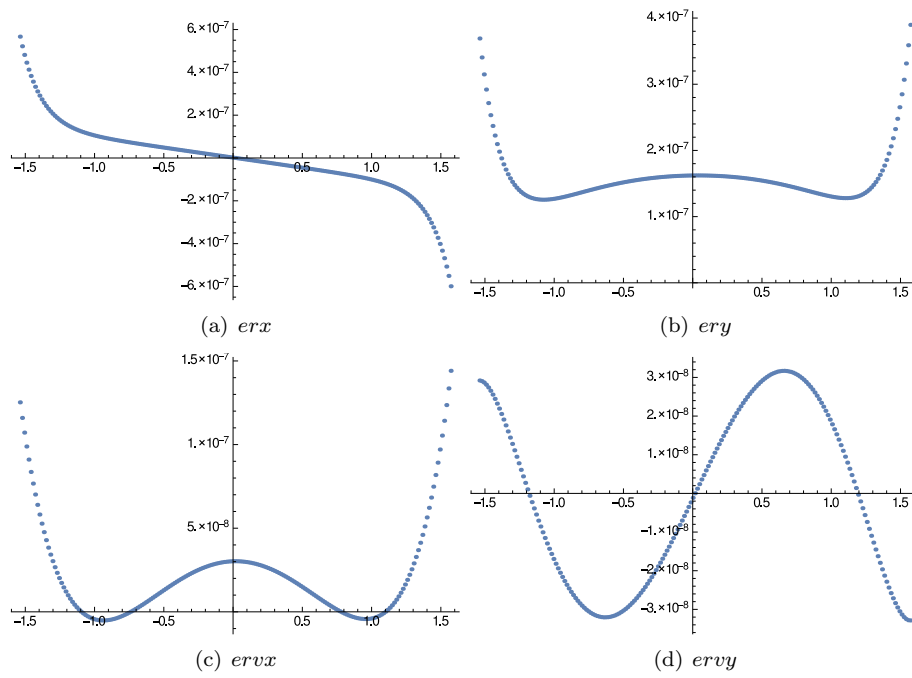
Figure 6: Local integration errors distribution $e = 1.05$, $f = \Psi_{1.00}$

14

(a) *erx*

(b) *ery*

(c) *ervx*

(d) *ervy*
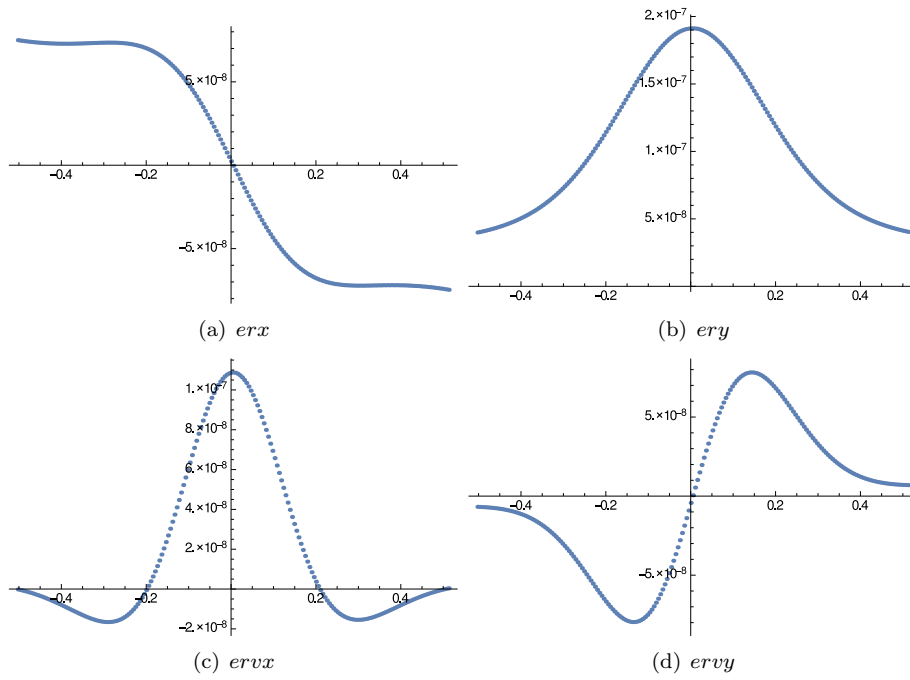
Figure 7: Local integration errors distribution $e = 1.05$, $\Psi_{2.00}$

15

(a) *erx*

(b) *ery*
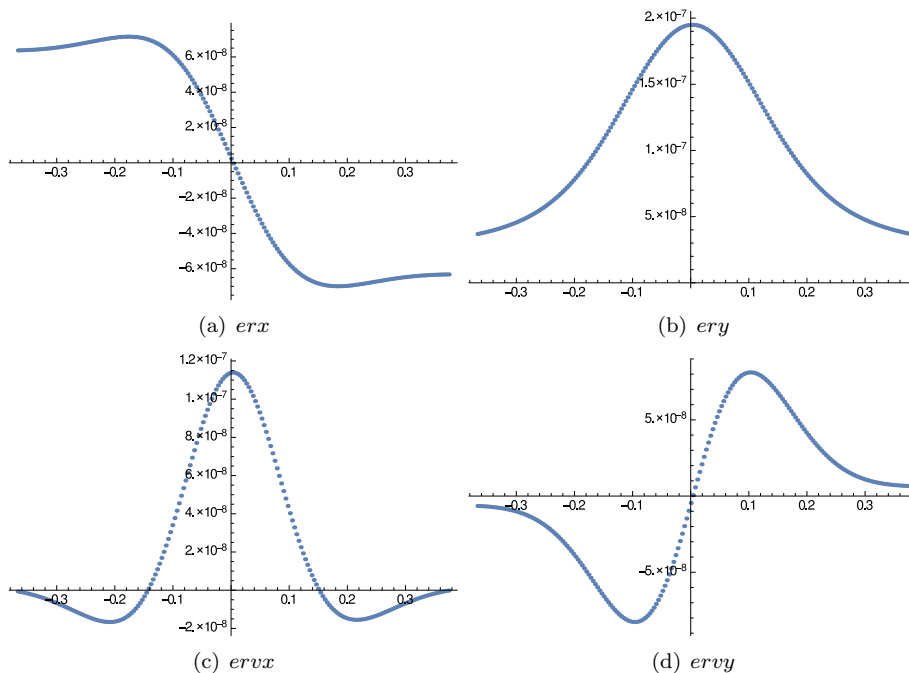
(c) *ervx*

(d) *ervy*

Figure 8: Distribution of the local integration errors $e = 1.05$, $\Psi_{5.00}$

5. Concluding Remarks

In this paper a new one-parametric family of anomalies, named as generalized geometric anomalies, has been defined.

The generalized eccentric family of anomalies includes the true anomaly. This family can be considered as defined by a family of hyperbolas $x^2/a^2 - y^2/b^2 = 1$ with the same major semiaxis and minor semiaxis given by $a\sqrt{\alpha^2 e^2 - 1}$ and the focus on $F_\alpha = -\alpha\, e\, a$.

It is very important to emphasize that the main quantities of the two body problem (position, velocity, vector radius, sinus and cosines of the eccentric anomaly) obtained in section 2, can be written in a closed form using the described family of anomalies.

This family can be extended to the repulsive forces in the form $F = \mu \frac{\vec{r}}{r^3}$ as in the case of two electric charges of the same sign. In this case the movement is a keplerian motion on the external branch of the hyperbola. We can also use this family of anomalies and the main quantities of motion can be obtained in closed form with respect to these anomalies.

It is also remarkable that the family of generalized family of geometric anomalies can be used to improve the integration errors in the numerical methods, although this is out of the scope of the paper. In this sense, two sets of numerical

studies have been developed, the first one through the study of the integration error for a large scale of time between two distant symmetrical points on the hyperbola. The positional errors decrease when the value of α increases. The second study shows the local truncation errors for an extreme case $e = 1.05$, We have also studied the local truncation error using several kinds of anomalies in the region limited by $f \in [-\pi/2, \pi/2]$.

6. Acknowledgements

[1] BROUWER, D.; CLEMENCE, G.M. 1965. *Celestial Mechanics*, Ed Academic Press, New York.

[2] BRUMBERG, E.V. 1992. Length of arc as independent argument for highly eccentric orbits. *Celestial Mechanics.* **53** 323–328.

[3] BRUMBERG, E.V., FUKUSHIMA, T. 1994. Expansions of Elliptic Motion based on Elliptic Functions Theory. ,*Celestial Mechanics.* **60**, 69-89.

[4] FERRÁNDIZ, J. M.; FERRER, S; SEIN-ECHALUCE, M.L. 1987. Generalized Elliptic Anomalies. *Celestial Mechanics.* **40.** 315–328

[5] JANIN, G. 1974. Accurate Computation of Highly Eccentric Satellite Orbits, *Celestial Mechanics.* **10**, 451–467.

[6] JANIN, G., BOND, V. R. 1980. The elliptic anomaly, *NASA Technical Memorandum 58228.*

[7] LÓPEZ, J. A.; MARCO, F. J., MARÍNEZ, M. J. 2014. A Study about the Integration of the Elliptical Orbital Motion Based on a Special One-Parametric Family of Anomalies. *Abstract and Appied Analysys. Volume 2014, Article ID 162060*

[8] LÓPEZ, J. A.; MARCO, F. J., MARÍNEZ, M. J. 2017. Geometrical definition of a continuous family of time transformations generalizing and including the classic anomalies of the elliptic two-body problem. *Journal of Computational and Applied Mathematics.* **309**, 482-492

[9] NACOZY, P. 1997. The intermediate anomaly. *Celestial Mechanics.* **16** 309–313.

[10] SUNDMAN, K. 1912.Memoire sur le probleme des trois corps, *Acta Mathematica* **36** 105–179.

[11] VELEZ, C. E.; HILINSKI, S. 1978., Time Transformation and Cowell's Method. *Celestial Mechanics.* **17** 83–99.